

# The evolution of the active phase in CoMo/C hydrodesulfurization catalysts under industrial conditions: a high-pressure Mössbauer emission spectroscopy study

A.I. Dugulan\*, M.W.J. Crajé, A.R. Overweg, G.J. Kearley

*Interfacultair Reactor Instituut, Delft University of Technology, Mekelweg 15, 2629 JB Delft, The Netherlands*

Received 9 July 2004; revised 19 October 2004; accepted 10 November 2004

Available online 22 December 2004

## Abstract

Mössbauer emission spectroscopy (MES) was used to study the influence of high pressure on the sulfidation of CoMo/C catalysts. During temperature stepwise treatment at 4 MPa the catalysts' behavior closely follows the Co–Mo–S model. The obtained MES spectra are different from those previously observed for CoMo/C catalysts sulfided under atmospheric pressure conditions, where the highly dispersed Co<sub>9</sub>S<sub>8</sub>-type structures are formed. It is suggested that the high-pressure conditions induce the binding of Co and Mo intermediate species, favoring Co–Mo–S phase formation. The results indicate that the contradictions between some catalyst models are partly related to the formation of different Co species upon different activation procedures. Lower stability compared with the alumina-supported catalysts was observed for the Co sulfide species in the CoMo/C catalysts under high-pressure sulfiding conditions. This can have important implications for the high-pressure stability of Type II Co–Mo–S, which is believed to have the same properties as the carbon-supported Co–Mo–S structures.

© 2004 Elsevier Inc. All rights reserved.

**Keywords:** Hydrodesulfurization; Mössbauer emission spectroscopy; High pressure; Co–Mo–S; Carbon

## 1. Introduction

Current specifications on sulfur content in transportation fuels amount to 150 mg/kg (parts per million) for gasoline and 350 ppm for diesel; both limits will be reduced to 50 ppm as of January 1, 2005. “Zero-sulfur” fuels (defined as having a maximum sulfur content of 10 ppm) will become mandatory in 2009 [1]. The continuing tightening of fuel quality standards has resulted in an increased need for the development of better performing hydrodesulfurization (HDS) catalysts.

Extensive research has been carried out on the CoMo hydrotreating catalysts, but the exact nature of the active phase and its mode of operation are still subjects of debate. Different structural models were proposed to explain the synergistic behavior of Co and Mo in HDS catalysts [2–5], but it

was only after the introduction of Mössbauer emission spectroscopy (MES) [6,7] that the Co–Mo–S structural model gained wide acceptance.

MES and extended X-ray absorption fine structure (EXAFS) measurements [8,9] revealed that the Co sulfide species that are located at the MoS<sub>2</sub> crystallite edges differ in particle size and/or ordering. The high thiophene HDS activity observed in carbon-supported Co (Co/C) catalysts, comparable to the activity of CoMo/C catalysts, led to the conclusion that the formation of a Co species like the one present in the Co–Mo–S structure does not necessarily require the presence of MoS<sub>2</sub> [10–13].

MES experiments have also shown the presence of a Co–Mo–S doublet in Co/C catalysts after sulfidation at 373 K, with the same parameters as for the CoMo/C catalysts sulfided at the same temperature [14,15]. After sulfidation at 673 K, the Co particles present in the Co/C catalyst sintered to a Co<sub>9</sub>S<sub>8</sub>-type phase, whereas CoMo/C showed a Co–Mo–S doublet with a lower quadrupole splitting (QS).

\* Corresponding author. Fax: +31 (0) 15 278 8303.

E-mail address: [i.dugulan@iri.tudelft.nl](mailto:i.dugulan@iri.tudelft.nl) (A.I. Dugulan).

EXAFS measurements [16] confirmed the similarities of the Co species in Co/C and CoMo/C catalysts sulfided at 373 K and suggested that the activity of CoMo/C catalysts arises from highly dispersed  $\text{CoS}_x$  particles stabilized by the secondary support  $\text{MoS}_2$ , which hinders sintering of this Co sulfide species. A structural model was proposed, in which part of the Co atoms, having a fourfold sulfur coordination, are present as very small  $\text{Co}_9\text{S}_8$ -type structures, and the rest of the Co atoms, having a sixfold sulfur coordination, are situated in a site in contact with Mo [16,17].

This model contradicted previous observations that the activity of CoMo/C catalysts should be related to the presence of Co–Mo–S structures [18,19].  $\text{H}_2$ – $\text{D}_2$  equilibration experiments also revealed that the sulfur atoms that bridge  $\text{Co}^{2+}$  and  $\text{Mo}^{4+}$  are very important for the activity of CoMo/C catalysts, indicating that  $\text{MoS}_2$  is part of the active component in HDS [20]. In addition, the promoting effect of  $\text{Co}_9\text{S}_8$  was associated with the fact that bulk Co sulfides can act as a support for highly dispersed Co-promoted  $\text{MoS}_2$ , as observed in unsupported CoMo sulfide catalysts [21]. A square-pyramidal model, in which fivefold sulfur-coordinated Co atoms in a tetragonal pyramid of sulfurs are situated on the  $\text{MoS}_2$  edges, was also suggested for the Co–Mo–S phase [22,23].

The influence of high pressure on the sulfidation of CoMo catalysts supported on alumina was recently studied by MES [24]; the complete sulfidation of Co atoms to the Co–Mo–S phase was observed. In this study we test the applicability of the Co–Mo–S structural model for carbon-supported catalysts activated under industrial conditions. Using a systematic temperature stepwise investigation of the sulfidation of CoMo/C catalysts, we examine the stability of the Co phases under high-pressure conditions. At the same time we try to relate the different contradicting structural information obtained in previous studies. The results are compared with those obtained with catalysts having the same metal loadings and prepared in the same way, sulfided under atmospheric pressure [25] and with the alumina-supported catalysts sulfided under high-pressure conditions [24].

## 2. Experimental

### 2.1. Catalyst preparation

Two CoMo catalysts were prepared by pore-volume impregnation, with activated carbon (Norrit RX3-extra; BET surface area  $1197 \text{ m}^2 \text{ g}^{-1}$ , pore volume  $1.0 \text{ ml g}^{-1}$ , particle size 0.5–0.85 mm) as a support material. Aqueous solutions of cobalt nitrate  $\text{Co}(\text{NO}_3)_2 \cdot 6\text{H}_2\text{O}$  (Merk, p.a.) and ammonium heptamolybdate  $(\text{NH}_4)_6\text{Mo}_7\text{O}_{24} \cdot 4\text{H}_2\text{O}$  (Merk, min. 99.9%) were used in a two-step impregnation procedure in which Mo was introduced first. About 50 MBq  $^{57}\text{Co}$  as an aqueous solution of  $\text{Co}(\text{NO}_3)_2 \cdot 6\text{H}_2\text{O}$  was added to the Co-containing impregnation solution for the MES measurements. After Mo introduction, the catalysts were

dried in static air at 383 K for 16 h, and after Co introduction the catalysts were left in static air at 293 K for 16 h. The two CoMo/C catalysts contained 7 wt% Mo; a high promoter-loading catalyst had 2.25 wt% Co [denoted  $\text{Co}(2.25)\text{Mo}(7)/\text{C}$ ], and a low promoter-loading catalyst had 0.04 wt% Co [denoted  $\text{Co}(0.04)\text{Mo}(7)/\text{C}$ ]. The catalyst loadings are given relative to the support material and are calculated from the impregnation solutions. The samples were sulfided in a flow of  $60 \text{ cm}^3 \text{ min}^{-1}$  of 10%  $\text{H}_2\text{S}/\text{H}_2$  mixture at 4 MPa in a high-pressure Mössbauer in situ reactor, similar to the reactor described in detail in [26]. This reactor offers the possibility of studying the catalysts under real industrial conditions. The applied sulfidation treatment is denoted (S,  $x$  MPa,  $y$  K), indicating that during the experiment the catalyst is linearly heated to  $y$  K at  $x$  MPa in 1 h and kept at that temperature for 1 h.

### 2.2. MES measurements

The MES spectra were recorded at room temperature and at the sulfiding pressure, with a constant acceleration spectrometer in a triangular mode with a moving single-line  $\text{K}_4\text{Fe}(\text{CN})_6 \cdot 3\text{H}_2\text{O}$  absorber enriched in  $^{57}\text{Fe}$ . The velocity scale was calibrated with a  $^{57}\text{Co}:\text{Rh}$  source and a sodium nitroprusside (SNP) absorber. Zero velocity corresponds to the peak position of the  $\text{K}_4\text{Fe}(\text{CN})_6 \cdot 3\text{H}_2\text{O}$  absorber measured with the  $^{57}\text{Co}:\text{Rh}$  source; positive velocities correspond to the absorber moving toward the source. The spectra were analyzed with a Lorentzian fitting procedure as described in [25].

## 3. Results

### 3.1. $\text{Co}(2.25)\text{Mo}(7)/\text{C}$

The Mössbauer spectra of stepwise sulfided  $\text{Co}(2.25)\text{Mo}(7)/\text{C}$  are presented in Fig. 1, and the resulting MES parameters are listed in Table 1. The spectrum of the fresh catalyst and the spectrum of the catalyst exposed to the sulfidation mixture before the pressure was increased are also presented.

Clearly, increasing the sulfidation pressure and temperature causes changes in the MES spectrum shape. The spectrum of the fresh catalyst consists of one quadrupole doublet, indicating a low-spin  $2+$  or a  $3+$  phase and a second contribution consistent with  $\text{Co}^{2+}$  in the high-spin state [27]. Exposure of the fresh catalyst to the  $\text{H}_2\text{S}/\text{H}_2$  gas mixture has an influence on the catalyst even at room temperature. The high-spin  $2+$  contribution decreases, but it does not disappear completely from the spectra until sulfidation at 573 K.

After treatment at 300 K, a second contribution with an isomer shift (IS) of  $0.18 \text{ mm s}^{-1}$  and a QS of  $1.21 \text{ mm s}^{-1}$  dominates the spectrum. The QS of this doublet remains constant after sulfidation at room temperature and 4 MPa, while it clearly depends on the subsequent increase in

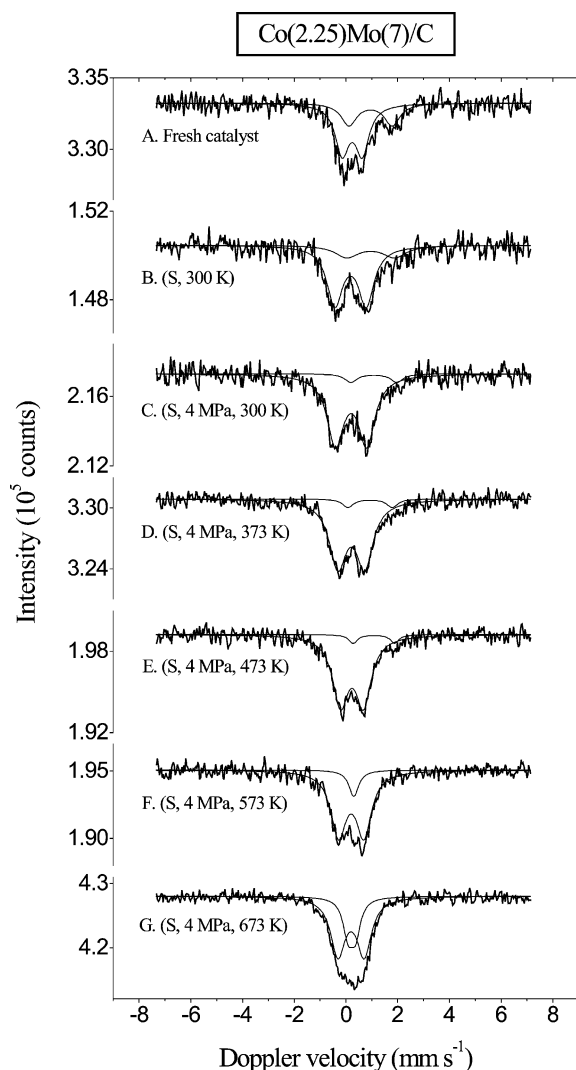


Fig. 1. MES spectra obtained at 300 K with the Co(2.25)Mo(7)/C catalyst after various successive sulfidation steps. Already after sulfidation at 573 K and 4 MPa the small QS doublet of sintered Co<sub>9</sub>S<sub>8</sub> is observed in the spectra.

Table 1  
MES parameters of Co(2.25)Mo(7)/C catalyst after sulfidation treatment

| $T_s$<br>(K)                   | $P$<br>(MPa) | Co-oxide                                 |  |  |                       | Co-sulfide                  |                             |                                   |          | High-spin 2+                |                             |                                   |          |
|--------------------------------|--------------|--|--|--|-----------------------|-----------------------------|-----------------------------|-----------------------------------|----------|-----------------------------|-----------------------------|-----------------------------------|----------|
|                                |              | IS <sup>a</sup><br>(mm s <sup>-1</sup> ) | QS <sup>b</sup><br>(mm s <sup>-1</sup> ) | $\Gamma$ <sup>c</sup><br>(mm s <sup>-1</sup> ) | A <sup>d</sup><br>(%) | IS<br>(mm s <sup>-1</sup> ) | QS<br>(mm s <sup>-1</sup> ) | $\Gamma$<br>(mm s <sup>-1</sup> ) | A<br>(%) | IS<br>(mm s <sup>-1</sup> ) | QS<br>(mm s <sup>-1</sup> ) | $\Gamma$<br>(mm s <sup>-1</sup> ) | A<br>(%) |
| Fresh                          |              | 0.25                                     | 0.77                                     | 0.65   | 66.3                  | –                           | –                           | –                                 | –        | 0.96                        | 1.67                        | 0.72                              | 33.7     |
| 300                            |              | –  | –  | –  | –                     | 0.18                        | 1.21                        | 0.74                              | 76.7     | 0.96                        | 1.85                        | 1.11                              | 23.3     |
| 300                            | 4            | –  | –  | –  | –                     | 0.20                        | 1.20                        | 0.78                              | 91.6     | 1.08                        | 1.78                        | 0.56                              | 8.4      |
| 373                            | 4            | –  | –  | –  | –                     | 0.21                        | 1.03                        | 0.80                              | 92.3     | 0.94                        | 1.71                        | 0.50 <sup>e</sup>                 | 7.7      |
| 473                            | 4            | –  | –  | –  | –                     | 0.24                        | 0.89                        | 0.74                              | 93.2     | 1.08                        | 1.6                         | 0.40                              | 6.8      |
| Co <sub>9</sub> S <sub>8</sub> |              |  |  |  |                       |                             |                             |                                   |          |                             |                             |                                   |          |
| 573                            | 4            | –  | –  | –  | –                     | 0.20                        | 0.98                        | 0.72                              | 88       | 0.30                        | –                           | 0.46                              | 12       |
| 673                            | 4            | –  | –  | –  | –                     | 0.20                        | 1.02                        | 0.68                              | 70.1     | 0.23                        | 0.29                        | 0.47                              | 29.9     |

<sup>a</sup> Isomer shift (IS):  $\pm 0.03$  mm s<sup>-1</sup>.

<sup>b</sup> Quadrupole splitting (QS):  $\pm 0.03$  mm s<sup>-1</sup>.

<sup>c</sup> Line width ( $\Gamma$ ):  $4 \pm 0.05$  mm s<sup>-1</sup>.

<sup>d</sup> Spectral contribution (A):  $\pm 5\%$ .

<sup>e</sup> Fixed during fit.

the sulfidation temperature. The QS value decreases to  $0.89$  mm s<sup>-1</sup> after high-pressure sulfidation at 373 and 473 K, but it increases during treatment at 573 and 673 K. At the same time, with the complete disappearance of the high-spin 2+ doublet, the spectrum of the Co(2.25)Mo(7)/C shows the presence of a new doublet, which after sulfidation at 673 K has an IS of  $0.23$  mm s<sup>-1</sup> and a QS of  $0.29$  mm s<sup>-1</sup>. This new doublet, assigned to sintered Co sulfide species, is already observed in the spectrum after treatment at 573 K, where, because of its relatively small spectral contribution, the MES parameters could not be derived precisely, and the resulting absorption line was fitted with only one singlet (see Fig. 1F).

### 3.2. Co(0.04)Mo(7)/C

Fig. 2 shows spectra of stepwise sulfided Co(0.04)Mo(7)/C catalyst; the corresponding fit parameters are presented in Table 2. The spectrum of the freshly prepared catalyst shows features similar to those of the Co(2.25)Mo(7)/C catalyst. The high-spin 2+ contribution almost doubles after exposure of the catalyst to the reaction mixture and disappears from the spectrum upon sulfidation at 473 K.

Again, the QS of the remaining doublet decreases to  $0.96$  mm s<sup>-1</sup> during treatment up to 473 K, and it increases after sulfidation at 573 and 673 K. The QS value of this doublet, after sulfiding at 673 K and 4 MPa, is larger than that obtained with the Co(2.25)Mo(7)/C catalyst treated in the same conditions. The small quadrupole doublet observed in the spectra of the high promoter-loading catalyst during sulfidation at higher temperatures is not observed with the Co(0.04)Mo(7)/C catalyst.

## 4. Discussion

Now that the first high-pressure in situ MES study on CoMo/Al<sub>2</sub>O<sub>3</sub> catalysts has shown that the Co–Mo–S model

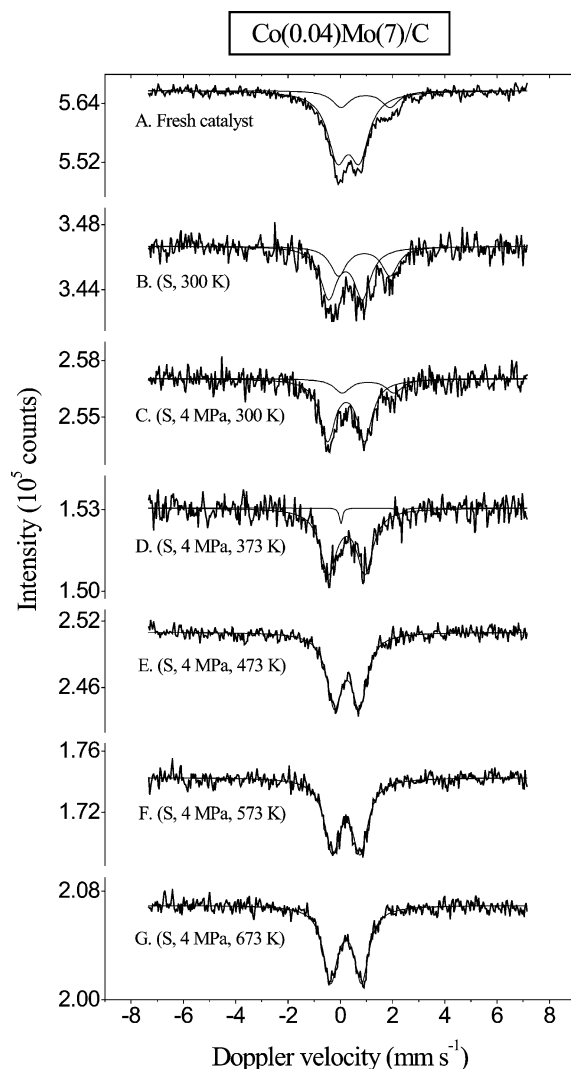


Fig. 2. MES spectra obtained at 300 K with the Co(0.04)Mo(7)/C catalyst after various successive sulfidation steps. The QS value of the dominant doublet increases during sulfidation at 573 and 673 K, indicating the redispersion of the Co-sulfide particles over the edges of MoS<sub>2</sub> crystallites.

is well suited for catalysts sulfided under industrial conditions [24], we now also want to know the influence of the pressure on our model system, carbon-supported catalysts. The main objective is to determine whether the highly dispersed Co sulfide particles are the active components also af-

ter high-pressure treatment, as observed for the atmospheric pressure sulfided catalysts [16], or Co is present in a unique phase together with MoS<sub>2</sub>, as indicated in the Co–Mo–S model.

The most impressive result, as observed in Fig. 1, is that the Co(2.25)Mo(7)/C catalyst sulfidation strictly follows the Co–Mo–S model. After activation the catalyst is characterized by a doublet with an IS of 0.20 mm s<sup>−1</sup> and a QS of 1.02 mm s<sup>−1</sup>, which can be assigned to a Co–Mo–S structure defined by the suggested MES parameters: IS = 0.22 mm s<sup>−1</sup> and QS = 1.0–1.3 mm s<sup>−1</sup> [28]. At the same time separate Co<sub>9</sub>S<sub>8</sub> structures are formed, as indicated by the same model for high Co/Mo ratios.

This behavior is completely different from the sulfidation trends observed with catalysts that have the same metal loadings and are prepared in the same way, treated under atmospheric pressure [25]. There a smaller doublet with a QS value of 0.88 mm s<sup>−1</sup> is obtained after sulfiding at 673 K. From combined MES and EXAFS measurements [16] this doublet was assigned to highly dispersed Co<sub>9</sub>S<sub>8</sub>-type structures, whose complete sintering to crystalline Co<sub>9</sub>S<sub>8</sub> is hindered by MoS<sub>2</sub>. The absence of a strong Co–Mo interaction induced separate sulfidation of the Co atoms during atmospheric pressure activation; the resulting Co sulfide species were located at a site in contact with MoS<sub>2</sub> [17]. Although the catalysts in the present study are not calcined, it is clear that upon high-pressure treatment, binding of Co and Mo atoms takes place and the sulfidation pattern follows the Co–Mo–S model.

These findings confirm the previous observations that the contradictions between the different catalyst models can be related to the fact that the promoter atoms are not always present in the Co–Mo–S structures [29,30]. Depending on the choice of activation conditions, highly dispersed Co<sub>9</sub>S<sub>8</sub>-type structures can also be formed.

The second striking result is the low stability of the Co–Mo–S structure in the Co(2.25)Mo(7)/C catalyst under high-pressure sulfiding conditions. Already after sulfidation at 573 K the contribution assigned to sintered Co sulfide species is observed in the spectrum. Upon treatment at 673 K the resulting doublet has a QS value of 0.29 mm s<sup>−1</sup>, very close to the value indicated for crystalline Co<sub>9</sub>S<sub>8</sub> (QS = 0.26 mm s<sup>−1</sup>) [6]. The weak interaction of the MoS<sub>2</sub> par-

Table 2  
MES parameters of Co(0.04)Mo(7)/C catalyst after sulfidation treatment

| $T_s$<br>(K) | $P$<br>(MPa) | Co-oxide                    |                             |                                   |          | Co-sulfide                  |                             |                                   |          | High-spin 2+                |                             |                                   |          |
|--------------|--------------|-----------------------------|-----------------------------|-----------------------------------|----------|-----------------------------|-----------------------------|-----------------------------------|----------|-----------------------------|-----------------------------|-----------------------------------|----------|
|              |              | IS<br>(mm s <sup>−1</sup> ) | QS<br>(mm s <sup>−1</sup> ) | $\Gamma$<br>(mm s <sup>−1</sup> ) | A<br>(%) | IS<br>(mm s <sup>−1</sup> ) | QS<br>(mm s <sup>−1</sup> ) | $\Gamma$<br>(mm s <sup>−1</sup> ) | A<br>(%) | IS<br>(mm s <sup>−1</sup> ) | QS<br>(mm s <sup>−1</sup> ) | $\Gamma$<br>(mm s <sup>−1</sup> ) | A<br>(%) |
| Fresh        |              | 0.31                        | 0.84                        | 0.90                              | 80.4     | –                           | –                           | –                                 | –        | 0.97                        | 1.88                        | 0.81                              | 19.6     |
| 300          |              | –                           | –                           | –                                 | –        | 0.20                        | 1.30                        | 0.76                              | 63.4     | 0.92                        | 1.97                        | 0.76                              | 36.6     |
| 300          | 4            | –                           | –                           | –                                 | –        | 0.23                        | 1.41                        | 0.70                              | 80       | 1.07                        | 1.98                        | 0.76                              | 20       |
| 373          | 4            | –                           | –                           | –                                 | –        | 0.25                        | 1.40                        | 0.76                              | 95.5     | 1.18                        | 2.30                        | 0.14                              | 4.5      |
| 473          | 4            | –                           | –                           | –                                 | –        | 0.26                        | 0.96                        | 0.67                              | 100      | –                           | –                           | –                                 | –        |
| 573          | 4            | –                           | –                           | –                                 | –        | 0.23                        | 1.06                        | 0.72                              | 100      | –                           | –                           | –                                 | –        |
| 673          | 4            | –                           | –                           | –                                 | –        | 0.22                        | 1.19                        | 0.67                              | 100      | –                           | –                           | –                                 | –        |



ticles with the inert carbon carrier leads, most probably, to the formation of relatively large  $\text{MoS}_2$  slabs with fewer edge positions to accommodate all Co atoms, and sintering of  $\text{Co}_9\text{S}_8$  occurs.  $\text{Co}_9\text{S}_8$  formation takes place faster than in the alumina-supported catalyst, with the same metal composition, also measured after high-pressure sulfidation [24].

It should be pointed out that the Mössbauer measurements do not provide direct information on the morphology of the  $\text{MoS}_2$  structures. The interpretation of the sintering of  $\text{Co}_9\text{S}_8$  in terms of a decreasing number of edge positions of  $\text{MoS}_2$  is in agreement with previous MES studies [45]. The decrease in the Mo edge dispersion, due to the lateral and three-dimensional growth of the  $\text{MoS}_2$  slabs, with increasing process severity was observed by means of different techniques [47]. An increase in the length of the  $\text{MoS}_2$  domains was also observed with increasing sulfidation pressure [48].

This low stability of the Co–Mo–S phase in the Co(2.25)Mo(7)/C catalyst can have important implications for the high-pressure stability of the Type II Co–Mo–S, in which all Mo–O–Al linkages with the support are completely sulfided [31], which is believed to have the same properties as the carbon-supported Co–Mo–S structures [32,33]. The high-pressure stability of Co–Mo–S II obtained with complexing agents [34–36] in uncalcined alumina-supported catalysts is particularly questioned.

These findings are intriguing, since the activity of CoMo catalysts supported on carbon was found to be higher than the activity of alumina-supported catalyst for both HDS reactions of dibenzothiophene (DBT) and 4,6-dimethyldibenzothiophene (4,6-DMDBT), as resulted from measurements performed under high-pressure conditions [37,38]. However, in those studies the catalyst activation was performed at atmospheric pressure and the activities were measured at a lower pressure (i.e., 2.9 MPa). The behavior of the highly dispersed  $\text{Co}_9\text{S}_8$ -type structures, which ought to be formed upon atmospheric-pressure presulfidation [16], after a subsequent increase in the reacting pressure, is not yet known. High activities were also measured at 4 MPa with CoMo/C catalysts calcined in a  $\text{N}_2$  atmosphere [39]. Binding of oxidic Co and Mo precursors during calcination can retard the catalyst sulfidation [40], delaying  $\text{Co}_9\text{S}_8$  segregation.

The spectra of both fresh Co(2.25)Mo(7)/C and Co(0.04)Mo(7)/C catalysts consist of two quadrupole doublets. The main spectral contribution, with an IS of  $0.25 \text{ mm s}^{-1}$  and  $0.31 \text{ mm s}^{-1}$ , respectively, is assigned to Co oxide species. The second contribution, representing a high-spin 2+ phase, does not completely disappear until sulfidation at 573 K for the high promoter-loading catalyst and 473 K for the low promoter-loading catalyst. This intermediate high-spin 2+ doublet must be assigned to oxygen-containing species, most probably a Co sulfate-type phase, as suggested by previous EXAFS measurements [16].

The temperature at which this high-spin 2+ phase is completely sulfided is higher for the high promoter-loading catalyst; this behavior is different from that observed with the same catalysts during atmospheric pressure sulfidation,

where with decreasing Co loading, a more severe sulfidation treatment is necessary to make such a phase disappear [25]. The presence of unsulfided Co atoms at temperatures as high as 473 K is also different from the atmospheric pressure-sulfided catalysts, when complete Co sulfidation was achieved at lower temperatures. The high-pressure treatment clearly retards the sulfidation of the intermediate high-spin 2+ phase.

For the low promoter-loading catalyst, after exposure to the  $\text{H}_2\text{S}/\text{H}_2$  gas mixture at room temperature, an increase in the spectral contribution of the high-spin 2+ phase is observed. This can be explained by removal of water associated with the high-spin 2+ species in the fresh catalyst, causing an increased interaction of these structures with the support [41]. The larger amount of unsulfided high-spin 2+ phase present at this stage, compared with the high promoter-loading catalyst, can also be understood in terms of formation of the intermediate Co sulfate-type phase, which is more difficult to sulfide in low promoter-loading catalysts under atmospheric-pressure conditions [25].

The MES parameters obtained after sulfidation at room temperature are different from those of the fresh catalyst; the main spectral contribution is assigned to Co sulfide species, as indicated by Crajé et al. [42]. The preferential adsorption of Co atoms to Mo during the preparation process allows the Co sulfidation to start at room temperature, even for the low promoter-loading catalyst [25].

During treatment at 573 and 673 K the QS of the dominant doublet increases, indicating a decrease in particle size and/or ordering of the Co sulfide species [25]. It was previously shown that Mo sulfidation takes place via a  $\text{MoS}_3$  phase, which transforms to  $\text{MoS}_2$  between 523 and 573 K [43]. In addition, the size of  $\text{MoS}_2$  crystallites was found to increase with increasing sulfiding temperature to 573 and 673 K [44]. Thus, the observed increase in the QS after treatment at 573 K can be understood in terms of redispersion of the Co sulfide particles over the edges of newly formed  $\text{MoS}_2$  crystallites. Since the Co(0.04)Mo(7)/C catalyst follows the same trend at exactly the same temperatures, it is concluded that the high-pressure conditions enhance the Co–Mo interactions favoring Co–Mo–S phase formation, also for the low promoter-loading catalysts.

The doublet that resulted from stepwise sulfidation of the Co(0.04)Mo(7)/C catalyst at 4 MPa and temperatures up to 673 K has MES parameters (IS =  $0.22 \text{ mm s}^{-1}$ , QS =  $1.19 \text{ mm s}^{-1}$ ) that are also characteristic of Co–Mo–S structures. The  $\text{Co}_9\text{S}_8$  doublet is not observed in the spectra of sulfided Co(0.04)Mo(7)/C catalyst, since the  $\text{Co}_9\text{S}_8$  sintering is shifted to higher temperatures with decreasing Co content [45]; the  $\text{MoS}_2$  edge sites are still sufficient to accommodate the low amount of Co atoms in this catalyst.

Observation of the  $\text{Co}_9\text{S}_8$  segregation only for the high promoter-loading catalyst indicates that the low stability of the Co–Mo–S phase is not related to a high-pressure instability of the Co sulfide species, but is related to the weak support interaction of the Co–Mo–S structures, resulting in

the formation of large MoS<sub>2</sub> slabs. Although the Co/Mo ratio of the Co(2.25)Mo(7)/C catalyst is rather high (i.e., 0.52) and sintering of Co<sub>9</sub>S<sub>8</sub> is expected with an increased sulfiding temperature, the loss of Co–Mo–S occurs faster in the carbon-supported catalyst, after activation at 573 K and 4 MPa, compared with the same catalyst supported on alumina, where only after 4 h of treatment at 673 K and 4 MPa the spectral contribution of Co<sub>9</sub>S<sub>8</sub> was observed [24].

It was previously shown [46] that for the CoMo/C catalysts sulfided under atmospheric-pressure conditions, the number of Co atoms associated with the Co sulfide species is varied over a large range with varying Co/Mo ratios; the small Co sulfide particles at the MoS<sub>2</sub> edges being the active element. During sulfidation under atmospheric-pressure conditions the Co sulfide species continuously sinter; the highly dispersed Co<sub>9</sub>S<sub>8</sub>-type structures being stabilized at the edges of the MoS<sub>2</sub> crystallites. Separate formation of the Co–Mo–S phase and sintered Co<sub>9</sub>S<sub>8</sub> was never observed in carbon-supported catalysts sulfided under atmospheric pressure.

Since the MES spectra of the Co/C and CoMo/C catalysts can be indistinguishable [16], we should also consider the possibility of the initial formation of the CoS<sub>x</sub> (Co<sub>9</sub>S<sub>8</sub>-like) structures that could be virtually converted to Co–Mo–S after treatment at higher temperatures, followed by the segregation of excess Co to form the Co<sub>9</sub>S<sub>8</sub> phase. The Co sulfide (CoS<sub>x</sub>) species formed in CoMo/C catalysts activated under atmospheric-pressure conditions are highly dispersed Co<sub>9</sub>S<sub>8</sub>-type structures with MES parameters that deviate from the values of crystalline Co<sub>9</sub>S<sub>8</sub> and resemble the Co–Mo–S parameters [16,46]. However, the transformation of these Co<sub>9</sub>S<sub>8</sub>-type structures into Co–Mo–S (by attaching to the MoS<sub>2</sub> edges) and crystalline Co<sub>9</sub>S<sub>8</sub> was never observed. For example, a catalyst having a much higher Co/Mo ratio—Co(4.3)Mo(7)/C—is still showing only the presence of the highly dispersed Co<sub>9</sub>S<sub>8</sub>-type species even after sulfidation at 673 K and atmospheric pressure [46], though one would expect there to be a much faster transition to Co–Mo–S and sintered Co<sub>9</sub>S<sub>8</sub>. This indicates that if the CoS<sub>x</sub> (Co<sub>9</sub>S<sub>8</sub>-like) structures are to be formed, they will continuously sinter to crystalline Co<sub>9</sub>S<sub>8</sub> and not disproportionate to form Co–Mo–S.

Treatment under high-pressure conditions, as in the present experiments, induces the binding of Co and Mo intermediate species and Co–Mo–S phase formation. The main quadrupole doublet in the spectrum of the Co(2.25)Mo(7)/C catalyst sulfided at 573 K and 4 MPa, with a QS value of 0.98 mm s<sup>−1</sup>, clearly reveals a Co–Mo–S structure, defined by QS values of 1.0–1.3 mm s<sup>−1</sup> [28]. Formation of the larger, highly dispersed Co<sub>9</sub>S<sub>8</sub>-type structures at the MoS<sub>2</sub> edges, characterized by smaller QS values (e.g., 0.88 mm s<sup>−1</sup> for the Co(2.25)Mo(7)/C catalyst sulfided under atmospheric pressure at 573 and 673 K [25]), is not observed in the present study.

The increase in the QS value of the Co sulfide species, observed for both Co(2.25)Mo(7)/C and Co(0.04)Mo(7)/C

catalysts during high-pressure activation at the temperature at which the MoS<sub>2</sub> crystallites are formed (i.e., 523–573 K), indicating a redispersion of the Co sulfide particles, confirms the Co–Mo–S phase formation. Upon treatment at 673 K and 4 MPa, the high promoter-loading catalyst is further deactivated, and sintering of the active species becomes more important at this stage than previously observed with the catalyst supported on alumina.

## 5. Conclusions

The influence of high pressure on the sulfidation of CoMo/C catalysts was studied by MES. The trends observed in the spectra after temperature stepwise treatment at 4 MPa resemble those seen for calcined CoMo/Al<sub>2</sub>O<sub>3</sub>, with the sulfidation closely following the Co–Mo–S model. This behavior is different from that of CoMo/C catalysts sulfided under atmospheric-pressure conditions, where the formation of the highly dispersed Co<sub>9</sub>S<sub>8</sub>-type structures takes place.

From the present results it is concluded that the high-pressure conditions induce the binding of Co and Mo intermediate species, favoring Co–Mo–S phase formation. The choice of activation conditions is very important: dispersed bulk Co sulfides can be formed instead of the desired Co–Mo–S structures.

Another important finding of this study is that the Co sulfide species has a lower stability in carbon-supported catalysts under high-pressure sulfiding conditions, compared with the alumina-supported catalysts. Already after sulfidation at 573 K and 4 MPa, Co<sub>9</sub>S<sub>8</sub> segregation occurs, faster than in the calcined alumina-supported catalysts treated in the same conditions. This raises doubts about the high-pressure stability of the Type II Co–Mo–S phase, since it is believed that Co–Mo–S structures on carbon have the same properties as the Type II structures.

## References

- [1] Directive 2003/17/EC of the European Parliament and of the Council—amending Directive 98/70/EC relating to the quality of petrol and diesel fuels.
- [2] B.C. Gates, J.R. Katzer, G.C.A. Schuit, in: *Chemistry of Catalytic Processes*, McGraw–Hill, New York, 1979, p. 411.
- [3] R.J.H. Voorhoeve, J.C.M. Stuver, *J. Catal.* 23 (1971) 243.
- [4] A.L. Farragher, P. Cossee, in: J.W. Hightower (Ed.), *Proceedings of 5th International Congress on Catalysis*, Palm Beach, 1972, North Holland, Amsterdam, 1973, p. 1301.
- [5] B. Delmon, in: H.F. Barry, P.C.H. Mitchell (Eds.), *Proceedings of 3rd International Conference on the Chemistry and Uses of Molybdenum*, Ann Arbor, 1979, p. 73.
- [6] H. Topsøe, B.S. Clausen, R. Candia, C. Wivel, S. Mørup, *J. Catal.* 68 (1981) 433.
- [7] C. Wivel, R. Candia, B.S. Clausen, S. Mørup, H. Topsøe, *J. Catal.* 68 (1981) 453.
- [8] M.W.J. Crajé, V.H.J. de Beer, A.M. van der Kraan, *Hyp. Int.* 69 (1991) 795.
- [9] M.W.J. Crajé, V.H.J. de Beer, J.A.R. van Veen, A.M. van der Kraan, *Appl. Catal. A* 100 (1993) 97.

- [10] J.P.R. Vissers, V.H.J. de Beer, R. Prins, *J. Chem. Soc., Faraday Trans.* 1 83 (1987) 2145.
- [11] V.H.J. de Beer, J.C. Duchet, R. Prins, *J. Catal.* 72 (1981) 369.
- [12] J.C. Duchet, E.M. van Oers, V.H.J. de Beer, R. Prins, *J. Catal.* 80 (1983) 386.
- [13] M.W.J. Crajé, V.H.J. de Beer, A.M. van der Kraan, *Appl. Catal.* 70 (1991) L7.
- [14] A.M. van der Kraan, M.W.J. Crajé, E. Gerkema, W.L.T.M. Ramselaar, V.H.J. de Beer, *Appl. Catal.* 39 (1988) L7.
- [15] A.M. van der Kraan, M.W.J. Crajé, E. Gerkema, W.L.T.M. Ramselaar, V.H.J. de Beer, *Hyp. Int.* 46 (1989) 567.
- [16] M.W.J. Crajé, S.P.A. Louwers, V.H.J. de Beer, R. Prins, A.M. van der Kraan, *J. Phys. Chem.* 96 (1992) 5445.
- [17] S.M.A.M. Bouwens, J.A.R. van Veen, D.C. Koningsberger, V.H.J. de Beer, R. Prins, *J. Phys. Chem.* 95 (1991) 123.
- [18] H. Topsøe, N.-Y. Topsøe, B.S. Clausen, in: *Proceedings of 12th Iberoamerican Symposium on Catalysis, Rio de Janeiro, vol. 2, 1990*, p. 762.
- [19] M. Breyse, B.A. Bennett, D. Chadwick, M. Vrinat, *Bull. Soc. Chim. Belg.* 90 (1981) 1271.
- [20] E.J.M. Hensen, G.M.H.J. Lardinois, V.H.J. de Beer, J.A.R. van Veen, R.A. van Santen, *J. Catal.* 187 (1999) 95.
- [21] K. Inamura, R. Prins, *Stud. Surf. Sci. Catal.* 92 (1995) 401.
- [22] W. Niemann, B.S. Clausen, H. Topsøe, *Catal. Lett.* 9 (1990) 355.
- [23] S.P.A. Louwers, R. Prins, *J. Catal.* 133 (1992) 94.
- [24] A.I. Dugulan, M.W.J. Crajé, G.J. Kearley, *J. Catal.* 222 (2004) 281.
- [25] M.W.J. Crajé, PhD thesis, Delft University of Technology, Delft, 1992, ISBN 90-73861-08-X.
- [26] M.W.J. Crajé, A.M. Van Der Kraan, J. van de Loosdrecht, P.J. van Berge, *Catal. Today* 71 (2002) 369.
- [27] J.G. Steven, L. Zhe, H. Pollak, V.E. Stevens, R.H. White, J.L. Gibson, *Mössbauer Handbook Minerals, Mössbauer Effect Data Center, University of North Carolina, Asheville, 1983*.
- [28] H. Topsøe, R. Candia, N.-Y. Topsøe, B.S. Clausen, *Bull. Soc. Chim. Belg.* 93 (1984) 783.
- [29] S. Eijssbouts, *Appl. Catal. A* 158 (1997) 53.
- [30] H. Topsøe, *J. Catal.* 216 (2003) 155.
- [31] R. Candia, O. Sorensen, J. Villadsen, N.-Y. Topsøe, B.S. Clausen, H. Topsøe, *Bull. Soc. Chim. Belg.* 93 (1984) 763.
- [32] H. Topsøe, B.S. Clausen, N.-Y. Topsøe, E. Pedersen, *I&EC Fundamentals* 25 (1986) 25.
- [33] H. Topsøe, B.S. Clausen, S. Mørup, *Hyp. Int.* 27 (1986) 231.
- [34] L. Medici, R. Prins, *J. Catal.* 163 (1996) 38.
- [35] L. Coulier, V.H.J. de Beer, J.A.R. van Veen, J.W. Niemantsverdriet, *J. Catal.* 197 (2001) 26.
- [36] E.J.M. Hensen, V.H.J. de Beer, J.A.R. van Veen, R.A. van Santen, *Catal. Lett.* 84 (2002) 59.
- [37] H. Farag, D. Whitehurst, K. Sakanishi, I. Mochida, *Catal. Today* 50 (1999) 9.
- [38] H. Farag, I. Mochida, K. Sakanishi, *Appl. Catal. A* 194–195 (2000) 147.
- [39] J.J. Lee, S. Han, H. Kim, J.H. Koh, T. Hyeon, S.H. Moon *Catal. Today* 86 (2003) 141.
- [40] A.F.H. Sanders, A.M. de Jong, V.H.J. de Beer, J.A.R. van Veen, J.W. Niemantsverdriet, *Appl. Surf. Sci.* 144–145 (1999) 380.
- [41] M.W.J. Crajé, E. Gerkema, V.H.J. de Beer, A.M. van der Kraan, *Hyp. Int.* 57 (1990) 1795.
- [42] M.W.J. Crajé, V.H.J. de Beer, A.M. van der Kraan, *Bull. Soc. Chim. Belg.* 100 (1991) 953.
- [43] M. de Boer, A.J. van Dillen, D.C. Koningsberger, J.W. Geus, *Jpn. J. Appl. Phys.* 32, Suppl. 32–2 (1993) 460.
- [44] T.G. Parham, R.P. Merrill, *J. Catal.* 85 (1984) 295.
- [45] R. Candia, B.S. Clausen, H. Topsøe, in: *Proceedings of 9th Iberoamerican Symposium on Catalysis, 16–21 July 1984, Lisbon, Portugal, 1984*, p. 211.
- [46] M.W.J. Crajé, V.H.J. de Beer, J.A.R. van Veen, A.M. van der Kraan, in: M.L. Occelli, R. Chianelli (Eds.), *Hydrotreating Technology for Pollution Control*, Dekker, New York, 1996, p. 95.
- [47] H. Topsøe, B.S. Clausen, F.E. Massoth, in: J.R. Anderson, M. Boudart (Eds.), *Hydrotreating Catalysts*, in: *Catal. Science Technol.*, vol. 11, Springer, Berlin, 1996.
- [48] P.J. Kooyman, J.G. Buglass, H.R. Reinhoudt, A.D. van Langeveld, E.J.M. Hensen, H.W. Zandbergen, J.A.R. van Veen, *J. Phys. Chem. B* 106 (2002) 11795.